Hindawi
Journal of Nanomaterials
Volume 2022, Article ID 4056551, 15 pages
https://doi.org/10.1155/2022/4056551

Research Article

Characterization Analysis of Silver Nanoparticles Synthesized from *Chaetoceros calcitrans*

R. Anith Jose,[1] **D. Devina Merin**,[2] **T. S. Arulananth**,[3] **and Nagaraju Shaik**[4]

[1]*Department of Electronics and Communication Engineering, Ponjesly College of Engineering, Nagercoil, Kanyakumari District, India*
[2]*Department of Biotechnology, Udaya School of Engineering, Vellamodi, Kanyakumari District, India*
[3]*Department of Electronics and Communication Engineering, MLR Institute of Technology, 500043, Hyderabad, Telangana, India*
[4]*College of Engineering and Technology, Wollega University, Nekemte, Ethiopia*

Correspondence should be addressed to Nagaraju Shaik; sknagaraju@wollegauniversity.edu.et

Received 6 August 2022; Revised 22 August 2022; Accepted 29 August 2022; Published 22 September 2022

Academic Editor: Deepanraj B

The marine microalgae *Chaetoceros calcitrans* were used in the synthesis of silver or argentum nanoparticles. The reduction of silver nitrate to silver nanoparticles is observed in marine microalgae. The silver nanoparticles have a good imperative role in technological fields. The synthesis of silver nanoparticles from marine microalgae is a green nanotechnological method. The silver nanoparticle characterization is then carried out. The presence of silver nanoparticles is confirmed by UV-Vis spectroscopy. Fourier transform infrared spectroscopy, atomic force microscopy, photoluminescence, and X-ray diffractometry were used for the characterization analysis of synthesized silver nanoparticles. The research on the antimicrobial activity of silver nanoparticles is made to analyze the antagonistic nature against pathogenic organisms.

1. Introduction

Nanotechnology is a contemporary technology where it allows the engineering of materials by altering their sizes, and this has increased the application of nanomaterial in vast areas. The optical properties and thermal and physicochemical properties exhibited by nanomaterials are unusual. The reduction of the size of particles from bulk material to nanosized particles leads to pronounced modifications in the physical properties of the particular material. Reduction in imperfections, spatial confinement, and an increase in surface energy are the characteristics that lead to varied physical properties of nanomaterial [1]. The application of nanomaterials, when combined with other substances, can be increased in manufacturing devices which reduce pollution and also in the production of alternate energy [2].

Biological methods employed the microorganism or the plant extract in the synthesis of nanoparticles, which is a simple and nontoxic method [3]. Before the introduction of the biological method, the synthesis of nanomaterials involves the use of noxious chemicals and some hazardous by-products produced as well. Hence, the search for a new biological method is made, and the term "green nanotechnology" is coined. The "green" method of particle synthesis is highly demanding [2]. The size, shape, and equal distribution of nanoparticles in a solution are affected by thermal energy [4]. The nanomaterials can be used as coatings and as intercalation material during the manufacture of electrical batteries [5] and also used as optical receptors [6]. Nanomaterials can be used as catalysts [7]. These vast applications made researchers turn to the biological method of nanoparticle synthesis [8]. The antimicrobial activities exhibited by metal nanoparticles are high against pathogenic organisms [9]. Nanocrystallites are produced from magnetotactic bacteria [10]. The diatoms or the algae are proven to synthesize nanomaterials [11]. The green technology of synthesizing silver nanoparticles evolved from these observations and inferences. The silver nanomaterial produced by marine

microalgae is green nanotechnology. Silver nanoparticles are broadly used in the nanotechnology field in various applications [12].

2. Materials and Methods

2.1. Parameters Monitored and Controlled in Algal Growth. The devices used for the culturing of algae are usually built with Pyrex or Corning glasses. The algal culture absorbs the inorganic carbon and converts it into organic matter by the photosynthesis mechanism. The source used in the photosynthesis mechanism is light energy, and it drives the full mechanism. The intensity of light has an imperative role in the growth of the culture. The light intensity is low in the algal culture when the density of algae is increased and also in depth, where the light penetration is very low. Eighteen hours of illumination is provided for the culture grown on a laboratory scale. Fluorescent lamps are used for illumination in laboratory-scale algal culture, and for a large scale, culture done in tanks got illuminated by sunlight.

Temperature is the next parameter which has an influence on the growth of algae. The temperature of 20°C to 27°C is maintained in laboratories. The pH of the culture is one of the important parameters to be monitored and controlled. The optimum pH for algal culture is 8.1 to 8.8, but it can tolerate a pH of 7 to 9.1. When a slight variation is there in pH, complete disturbance happens in the culture and everything gets collapsed. Hence, great care is taken to maintain the pH of culture.

The sedimentation of culture that happens during algal culture is avoided by mixing. Mixing also helps the cells to get equally exposed to nutrients and illuminations and avoid stress on it. The mixing of algal culture is done by stirring the culture devices with hands, using aerators, using paddle wheels, and using an incubator shaker. The carbon source is made available in media, but also the fixation increases when the carbon source is supplied as carbon dioxide. This increases the growth of algae quickly. The air provided is sterilized by passing through a filter. The contaminating particles entering the culture media are avoided by using this technique.

Seawater is used for the culture to maintain the salinity of culture. The algae that are grown in salinity slightly less than their natural habitat grow well compared to the native one. Hence, a very little amount of normal water is mixed with seawater and diluted. This water is used for culture.

2.2. Algal Culture. The algal culture *Chaetoceros calcitrans* was brought from the Central Marine Fisheries Research Institute, Tuticorin, Tamil Nadu, India. The stock cultures were maintained and cultivated by using Walne's culture media. 20°C of temperature and 8.5 pH were provided to maintain the stocks. The algal cultures were illuminated for 24 hrs with fluorescent lamps. Every day, the growth of algal culture is checked and diluted appropriately when it was needed. Haffkine flasks were used for the mass culturing of algae. The media used in the mass cultivation of algae were Walne's media. Convenient aerations, low-level light intensity, 20°C of temperature, and 8.5 pH were made available for the mass production of algae. The cells are harvested when the required cell density was reached. 100 ml of each algal culture is grown separately to study the growth pattern of algae. Each alga's maximum absorbance is analyzed. The optical density of each alga is observed every 24 hrs. The analysis of the variation method was done to find the significant variation between the algal growths. Table 1 explains Walne's media.

The algal culture done on the laboratory scale is given in Figure 1.

2.3. Microscopical Identification. The algae *Chaetoceros calcitrans* maintained in the stock solution are then viewed microscopically. The nomenclature of *Chaetoceros calcitrans* is given below.

2.4. Nomenclature of Chaetoceros calcitrans. Chaetoceros is the most diverse genus of marine planktonic diatoms, with over 400 species described. In girdle view, cells are roughly rectangular. In valve view, cells are typically elliptical. Near their origin, opposing sets of adjacent cells touch.

(i) Kingdom: *Chromalveolata*

(ii) Phylum: *Heterokontophyta*

(iii) Class: *Bacillariophyceae*

(iv) Order: *Centrales*

(v) Family: Chaetocerotacae

(vi) Genus: *Chaetoceros*

  (a) Specific descriptor: *calcitrans*

  (b) Scientific name: *Chaetoceros calcitrans*

2.5. Synthesis of Silver Nanoparticles. Silver nanoparticles are synthesized from marine microalgae using two methods: normal marine microalgae and microwave irradiated marine microalgae.

2.5.1. Normal Marine Microalgae

(1) Synthesis of Silver Nanoparticles from Normal Marine Microalgae. The algal cultures from the midexponential phase of their growth are collected for the synthesis of nanoparticles, and the experiments are carried out in six methods. Control experiments have been carried out for all methods to determine the responsibility of algae in the production of silver nanoparticles.

(2) Synthesis of Silver Nanoparticles from Normal Marine Microalgal Culture along with 1 mM $AgNO_3$ Solution. The algae are grown in this method with 1 mM $AgNO_3$ solution. Initially, a 10% inoculum of *C. calcitrans* was being added to flasks containing seawater with normal Walne's media, followed by an equal amount of 1 mM silver nitrate solution. It was then shaken for two weeks to continue the synthesis by placing the solutions in a shaker.

(3) Synthesis of Silver Nanoparticles from the Microalgal Supernatant and Pellet. The algal cultures collected in the middle of the exponential phase are centrifuged for 5 minutes at 1000 rpm [26]. Then, the supernatants of 10 ml

Table 1: Composition of Walne's media.

Solution	Walne's media		The volume of solutions used for the algal cultivation of 100 ml
A	Potassium nitrate Sodium Orthophosphate EDTA (Na) Boric acid Ferric chloride Manganese chloride Distilled water	100 g 20 g 45 g 33.4 g 1.3 g 0.36 g 1 l	55 μl
B	Zinc chloride Cobalt chloride Copper sulfate Ammonium molybdate Distilled water	4.2 g 4.0 g 4.0 g 1.8 g 1 l	50 μl
C	Vitamin B_1 (thiamine) VitaminB_{12} (cyanocobalamine) Distilled water	200 mg 10 mg 100 ml	25 μl

Figure 1: Algal culture done in Walne's media.

of each algal culture are transferred to test tubes and the pellets are collected in separate test tubes, and then add 10 ml of $AgNO_3$ solution to each algal supernatant and the respective pellets and retain them in a shaking machine for two weeks to carry out synthesis and develop the color change.

(4) Synthesis of Silver Nanoparticles from Ultrasonicated Marine Microalgal Culture. About 10 ml of each algal culture collected in the middle of the exponential phase is ultrasonicated for about 5 mins at 600 rpm. Then, to each ultrasonicated algal culture, add 10 ml of $AgNO_3$ solution and keep it in a shaker for two weeks for synthesis [27].

(5) Synthesis of Silver Nanoparticles from the Ultrasonicated Microalgal Supernatant and Pellet. The algal culture collected in the middle of the exponential phase is ultrasonicated for about 5 mins and centrifuged at 1000 rpm for 5 mins. Then, the supernatants of 10 ml of each algal culture and the respective pellets are transferred to test tubes, and then add 10 ml of $AgNO_3$ solution to each algal supernatant and pellet. The tubes are kept in a shaker for two weeks to develop the color change.

Table 2: The rate of growth of *C. calcitrans* at 470 nm.

Day	*C. calcitrans* (optical density at 470 nm)
1	0.02
2	0.06
3	0.10
4	0.13
5	0.19
6	0.25
7	0.32
8	0.34
9	0.36
10	0.37
11	0.39
12	0.41
13	0.45
14	0.46
15	0.50
16	0.50
17	0.49
18	0.48
19	0.47
20	0.40
21	0.36
22	0.31
23	0.29
24	0.29
25	0.25
26	0.21
27	0.17
28	0.12
29	0.09
30	0.03

2.5.2. Microwave Irradiated Algal Culture

(1) Synthesis of Silver Nanoparticles from Microwave Irradiated Marine Microalgae. For the synthesis of nanoparticles, an algal culture in its midexponential phase was collected and microwave irradiated for 5 seconds on and 15 seconds off 5 times. Furthermore, the experiments were carried out using six different methods. Control experiments were carried out for all methods to determine the role of algae in the production of silver nanoparticles.

(2) Synthesis of Silver Nanoparticles from Microwave Irradiated Microalgal Culture along with 1 mM $AgNO_3$ Solution. In this method, the microwave irradiated algae are cultivated along with 1 mM $AgNO_3$ solution. A microwave irradiated algal inoculum of 10% is added to respective flasks

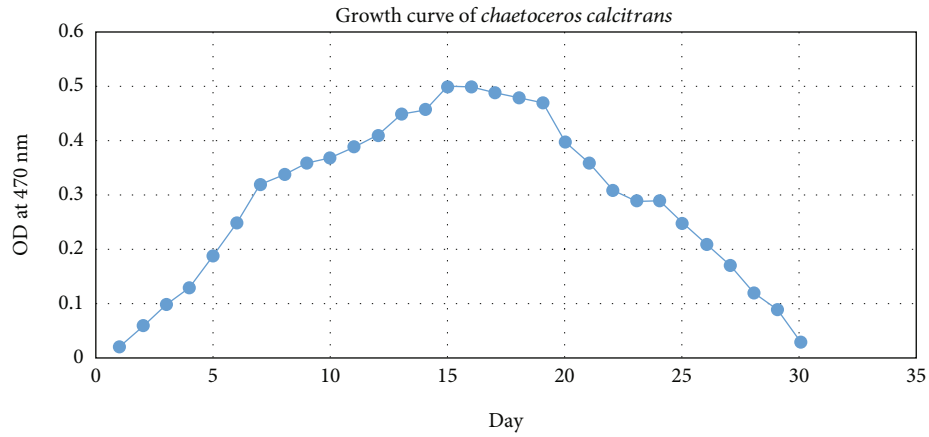

Figure 2: Growth curve of *C. calcitrans*.

Figure 3: Synthesis of silver nanoparticles from microalgae.

containing seawater with media, and then 10 ml of 1 mM silver nitrate solution was added and kept in a shaking machine for two weeks.

(3) Synthesis of Silver Nanoparticles from the Microwave Irradiated Microalgal Supernatant and Pellet. The microwave irradiated algal cultures collected in the middle of the exponential phase are centrifuged at 1000 rpm for 5 mins. The supernatant and pellet of each alga are taken in separate test tubes and added 10 ml of 1 mM silver nitrate solution and then kept in a shaker for two weeks.

(4) Synthesis of Silver Nanoparticles from Microwave Irradiated and Ultrasonicated Microalgal Culture. The microwave irradiated algal culture collected in the middle of the exponential phase is ultrasonicated for about 5 mins at 600 rpm. Then, to each ultrasonicated algal culture, add 10 ml of $AgNO_3$ solution and keep it in a shaker for two weeks.

(5) Synthesis of Silver Nanoparticles from the Microwave Irradiated and Ultrasonicated Microalgal Supernatant and Pellet. The microwave irradiated algal culture collected in the middle of the exponential phase is ultrasonicated for about 5 mins at 600 rpm and centrifuged at 5000 rpm for 5 mins. The supernatant and pellet of each algal culture are transferred to separate test tubes, and 10 ml of 1 mM silver nitrate solution is added and kept in a shaker for two weeks to identify and analyze the color changes.

2.6. Characterization of Silver Nanoparticles. The characterization study of silver nanoparticles is done to confirm the presence of silver nanoparticles and to analyze their size, shape, and other characteristic features.

2.6.1. UV-Vis Spectroscopy. UV-Vis spectroscopy is used to characterize and confirm the presence of reduced silver ions as silver nanoparticles in the algal culture. The wavelength range used for taking absorbance is from 200 nm to 700 nm. Both the UV range and the visible range are present in UV-Vis spectroscopy.

2.6.2. Scanning Electron Microscopy. The size details regarding the nanoparticle are obtained using scanning electron microscopy. The magnifications that can be done in scanning electron microscopy range from 20x to 30,000x. The area that ranges from 1 cm to 5 μm can be imaged. The colloidal solutions containing the silver nanoparticles are centrifuged at 5000 rpm for 12 minutes, and the supernatant is again centrifuged at 20,000 rpm to get pellets. These pellets are dissolved in an ionic solution and then photographed.

2.6.3. Transmission Electron Microscopy. The particle distribution and the size profile of distributed particles are analyzed using TEM. The TEM uses an electron beam to make a photograph of the image kept for identification. The silver nanoparticles obtained by the reduction process are prepared in such a way that they withstand the electron beam passing through them to make an image. The image obtained from TEM helps to make data regarding the silver nanoparticles.

2.6.4. Fourier Transform Infrared Spectroscopy. The chemical architecture of silver nanoparticles is studied using the FTIR spectrometer. The solution of nanoparticles is dried at 75°C, and the powder obtained is characterized in the range 4000 to 500 cm^{-1}.

2.6.5. Atomic Force Microscopy. Atomic force microscopy is used to investigate the presence of atoms on the surface of nanoparticles. The surface chemistry of nanoparticles can be analyzed thoroughly using AFM.

2.6.6. X-Ray Diffractometry. The size and nature of silver nanoparticles are studied by the graphical data obtained from XRD. Scherrer's formulas are used in XRD to interpret the

Figure 4: Synthesis of silver nanoparticles after microwave irradiation.

Table 3: Amount of silver nanoparticles synthesized from normal marine microalgae.

Sl. no.	Algae	Normal algae			Ultrasonicated algal culture		
		Algal culture (mg)	Algal supernatant (mg)	Algal pellet (mg)	Algal culture (mg)	Algal supernatant (mg)	Algal pellet (mg)
1	*C. calcitrans*	6.000	1.011	3.123	8.231	3.201	2.587

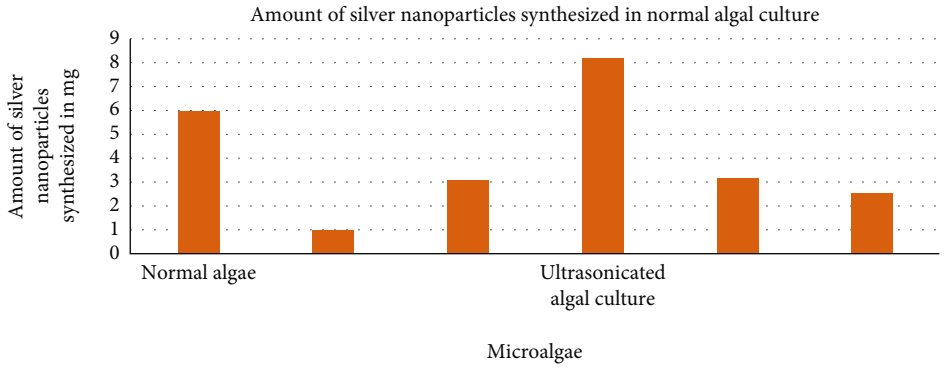

Figure 5: Amount of silver nanoparticles synthesized in normal algal culture.

Table 4: Amount of silver nanoparticles synthesized from microwave irradiated marine microalgae.

Sl. no.	Algae	Microwave irradiated algae			Microwave irradiated and ultrasonicated algal culture		
		Algal culture (mg)	Algal supernatant (mg)	Algal pellet (mg)	Algal culture (mg)	Algal supernatant (mg)	Algal pellet (mg)
1	*C. calcitrans*	9.154	2.315	3.545	12.335	4.257	2.978

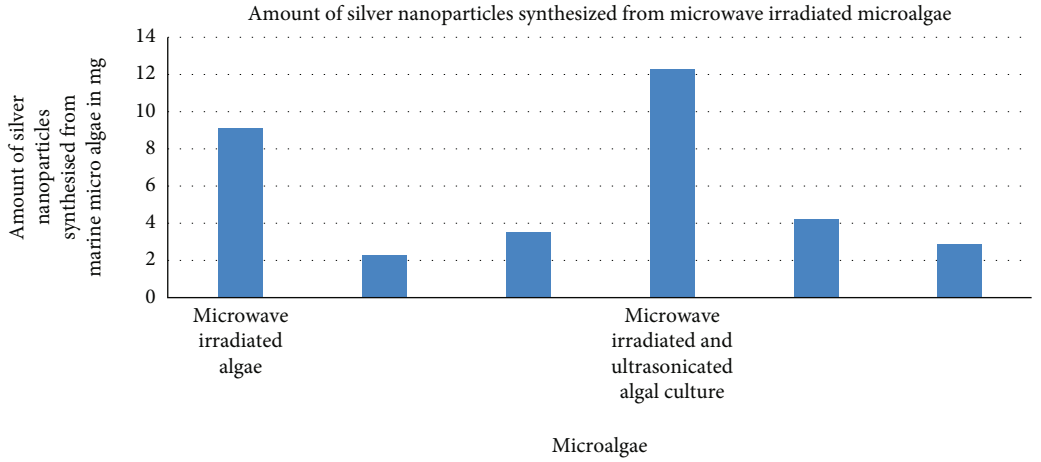

Figure 6: Amount of silver nanoparticles synthesized from microwave irradiated microalgae.

Figure 7: Silver nanoparticles in powdered form.

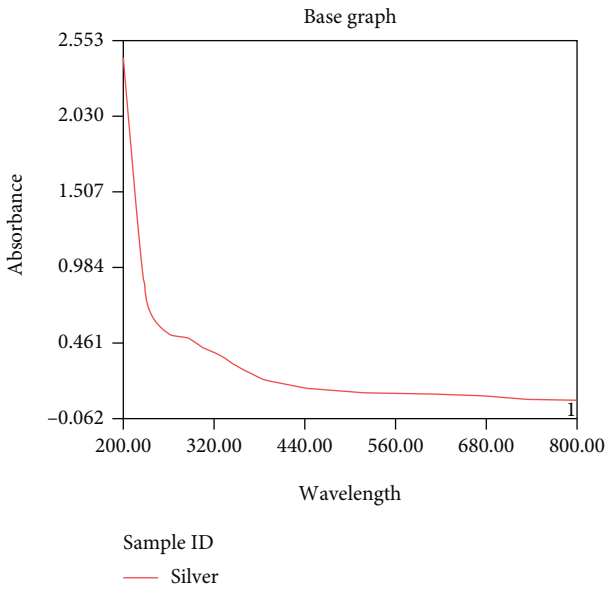

Figure 8: UV-Vis spectroscopy of silver nanoparticles.

results of XRD. The silver nanoparticles are ground to obtain a fine powder and then used in the XRD experiment.

2.6.7. Photoluminescence. The photoluminescence study is done to know the photon excitations of silver nanoparticles. A powdered sample of nanoparticles is used for the experimental data interpretation.

2.7. Antimicrobial Activity of Silver Nanoparticles. The antagonistic nature of silver nanoparticles against human pathogenic organisms is studied. The data are collected regarding the zone of inhibition obtained by silver nanoparticles against each human pathogenic organism. *A. niger*, *Enterobacter spp.*, *E. coli*, *Klebsiella spp.*, *P. vulgaricus*, *P. aeruginosa*, and *S. aureus* are human pathogenic organisms used to evaluate the opposing nature of silver nanoparticles.

3. Results and Discussion

The algal species *Chaetoceros calcitrans* are collected from the Central Marine Fisheries Research Institute (CMFRI), Tuticorin, Tamil Nadu, India. The stock is maintained in Walne's media. Walne's media are specially designed for the growth of marine microalgae by Walne in 1970. The algae were microscopically identified as *Chaetoceros calcitrans*. The mass cultivation of algae is done in Haffkine flasks. Each alga's growth was studied by measuring absorbance values at their respective maximum values. For the first 15 days, algal cells are in the exponential phase. After 15 days of growth, algal cells reach the stationary phase and begin to decline.

The λmax values for the microalgae are found using the Beer-Lambert law. The maximum absorbance for the marine microalgae *C. calcitrans* is 470 nm.

3.1. Dynamics of Algal Growth. An axenic culture of microalgae grows in five stages. Growth is usually associated with culture changes instead of just changes in an individual organism. The term "growth" refers to an increase in number beyond what was present in the original inoculums. In algal multiplication, there are five distinct stages of growth. The period after adding inoculums to a culture medium, when the population remains temporarily unchanged, is known as the lag phase. The size of algae grows beyond the normal dimensions. They are very active physiologically and are synthesizing new protoplasm. Although the organisms are metabolizing, cell division is slow. The cells divide at a constant rate during the next logarithmic or exponential phase. At this stage, the growth rate is at its peak under optimal culture conditions. When nutrients, light, pH, carbon dioxide, or other physical and chemical factors begin to limit growth, cell division starts to slow. The logarithmic phase of growth begins to taper off gradually after several hours or days in the stationary phase. For a time, the population remains relatively constant, possibly as a result of the complete withdrawal of division or the stabilizing of the regenerative capacity by an equivalent death rate. The final phase is the phase of decline or death, in which the rate at which some cells die exceeds the process at which new cells reproduce. The number of viable cells decreases in a straight line.

3.2. Data Analysis of Growth Dynamics of Algae. The growth dynamics of marine microalgae are analyzed for 30 days. The absorbance of each alga is noted at their λmax on a daily basis. The cells first undergo a lag phase where the multiplication of cells is not found, but the unicellular alga finds its adaptability to the new environment and then shows multiplication in its next phase. The exponential phase is the active phase of the alga, where it is multiplied and the cell number increases. Due to an increase in the cell number in the culture, the density, turbidity, and viscous nature of culture increase. The dense nature of culture gives an elevated absorbance for the exponential phase of algae.

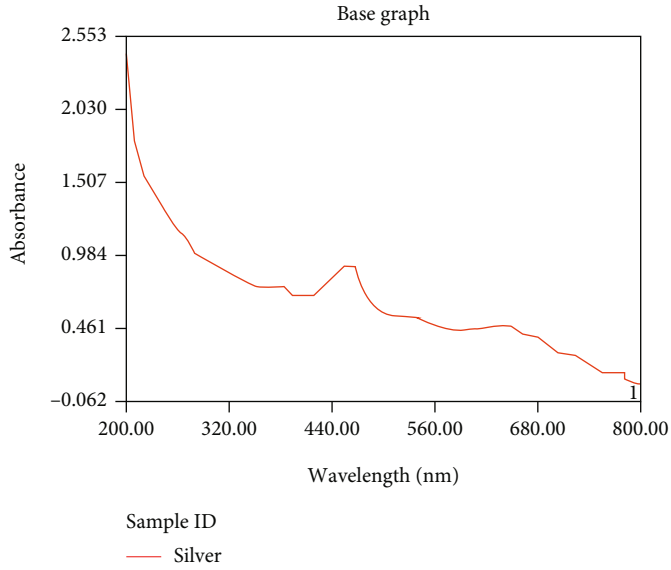

Figure 9: UV-Vis spectroscopy analysis of silver nanoparticles synthesized from microalgae *C. calcitrans*.

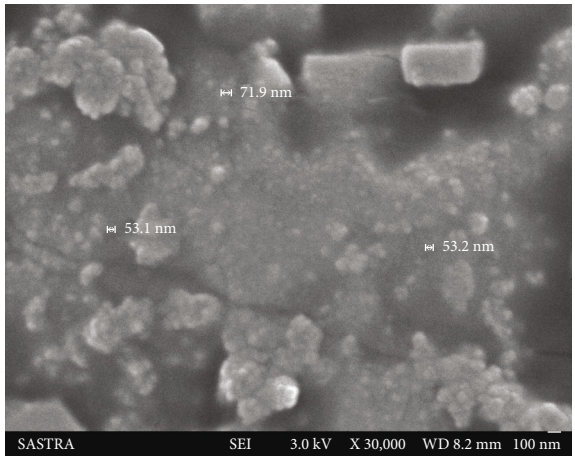

Figure 10: SEM image of nanoparticles with sizes 53 nm and 72 nm.

The microalgae reached the end of the exponential phase nearer to the 15th day, and the next phase, the stationary phase, starts. In the stationary phase, the cells remain stagnant without any multiplication due to the lack of availability of nutrients. The start of the stationary phase varied between species from 14 to 16 days. About 860×10^4 cells/ml of *C. calcitrans* are counted at the near end of an exponential phase in the marine microalgae. The algal culture at the near end of the exponential phase is used as a stock culture for the preparation of other pure cultures. The presence of marine microalgae is necessary for the balance nature of the environment since the photosynthesis process occurs at a higher rate during the exponential phase of growth, therefore reducing the carbon dioxide concentration in the environment [13]. The absorbance of algae observed for 30 days is given in Table 2.

The growth curve of *C. calcitrans* in normal nitrogen content in Walne's media is shown in Figure 2. The multiplication of *C. calcitrans* in normal nitrogen content in Walne's media showed a steep increase for 15 days and remained there in the stationary phase for 2 days and then declined. During the decline phase, cell death is not in a regular fashion but showed again a stationary phase and then declined.

3.3. Synthesis of Silver Nanoparticles. The presence of reddish brown-black color in the solution indicated the synthesis of silver nanoparticles. Due to the excitation of surface plasmon resonance and SPR bands, the solution with silver nanoparticles changes its color to brown color. The silver nanoparticles demonstrated high absorbance at 420 nm, which is the maximum absorbance demonstrated by silver particles. The color of synthesized nanoparticles was due to the surface plasmon excitation phenomenon. The size of nanoparticles also has an impact on color formation. When nanoparticles are of very small size and not aggregated, the color was yellow and turns to dark brown by the formation of larger molecules and the aggregation process that happens in the solution. The metabolites excreted by the silver-exposed culture could reduce silver ions, indicating that the reduction of the ions occurs via electron shuttles or through reducing agents released into the solution in the algal culture. These reactions took place only in the presence of light, and nanoparticles are not formed in the absence of light. The reduction process of bulk silver material to nanomaterial was analyzed [14]. The change in color acts as the primary confirmation test in silver nanoparticle synthesis [15–17]. Among the green metallic nanoparticles, silver nanoparticles were more preferable for the analysis of antimicrobials [18]. It has an oligodynamic action that allows it to bond to biomolecule membranes and aggregate the cell wall of bacteria [19]. The controls were maintained to carry out the experiment. The presence of flavonoids, alkaloids, saponins, tannins, quinones, and reducing sugars present in the alga itself acts as a capping and reducing agent. Hence, the addition of any other

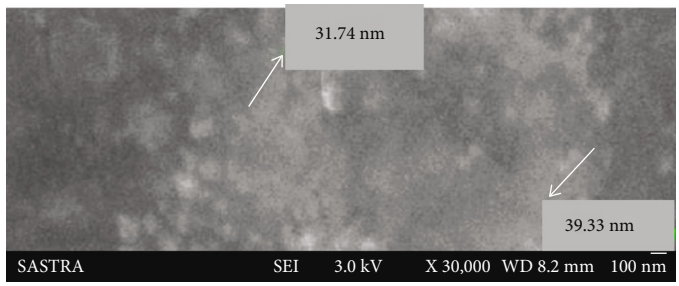

Figure 11: SEM image of nanoparticles with sizes 33 nm and 39 nm.

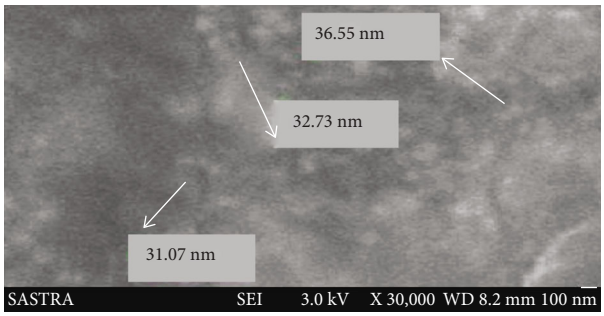

Figure 12: SEM image of nanoparticles with sizes 31 nm, 32 nm, and 36 nm.

chemicals is not needed which made the experiment eco-friendly. The silver nanoparticles synthesized from *C. calcitrans* by eco-friendly methodology remained stable for more than six months when stored at room temperature. The durability increases when preserved at a cool temperature.

The amount of silver nanoparticles synthesized in ultrasonicated algal culture is high compared to others since due to disturbance produced in the cell wall of microalgae (Figure 3), the reducing particles are released in the culture environment, and hence, many silver particles get reduced to silver nanoparticles. A trace amount of silver nanoparticles can be found in the supernatant and pellet due to the occurrence of reducing ions present. The temperatures have a great impact on the synthesis of silver nanoparticles. The temperature significantly affects the synthesis, formation, size, and shape of nanoparticles. By varying the temperature, the silver nanoparticles of the required shape and size can be obtained.

The occurrence of silver nanoparticles is given in Figure 4.

The amount of silver nanoparticles produced from normal marine microalgae is given in Table 3. The amount of silver nanoparticles synthesized by *C. calcitrans* in normal algal culture is 6 mg, and when ultrasonicated, it increases to 8.231 mg.

The amount of silver nanoparticles synthesized by *C. calcitrans* in normal algae and in ultrasonicated algal culture is graphically given in Figure 5.

The marine microalgae, when exposed to microwave irradiation, get stimulated to synthesize more silver nanoparticles than the normal microalgae, and it is given in Table 4. This is due to the reducing ions that get induced, and their release outside the cell is higher, and hence, more silver nanoparticles get synthesized. The quantity of synthesizing silver nanoparticles of microalgae can be improved by microwave irradiation for 5 sec on and 15 sec off 5 times. The amount of silver nanoparticles synthesized by *C. calcitrans* is 6.000 mg in normal which is improved to 9.154 mg by microwave irradiation.

The amount of silver nanoparticles synthesized from microwave irradiated marine microalgae is given in Figure 6.

The silver nanoparticles synthesized from microalgae can be dried and made into powder. The synthesized nanoparticles were collected after centrifugation as pellets and air-dried for 1 hour. Then, it was exposed to 100°C until the water content from the nanoparticles gets removed. The agglomerated particles were mechanically crushed to bring them to a fine powdered form. The nanoparticle powders are separated in Eppendorf tubes according to their different sizes after taking an SEM image. The powdered sample of nanoparticles is shown in Figure 7. The powdered form of silver nanoparticles is used in experiments.

3.4. UV-Visible Spectroscopy. The synthesis of silver nanoparticles in the algal culture is confirmed by taking its absorbance value using UV-Vis spectroscopy since silver nanoparticles exhibit their maximum absorbance in the UV range. The absorption and scattering efficiency of silver nanoparticles are very great. Their strong interaction with light occurs because when excited by light at specific wavelengths, the conduction electrons on the metal surface undergo a collective oscillation. Silver nanomaterial optical properties such as absorption, transmission, reflection, and light emission are dynamic and may differ significantly from bulk material properties.

The UV absorption spectra of the silver nanoparticle solution show the absorption peak in the visible range of 335.9 nm, as shown in Figure 8. In the graph, it shows that the sample silver nanoparticles have a strong absorption peak.

The UV-Vis spectroscopy is taken for all the silver nanoparticles synthesized from marine microalgae. The peak is obtained in the range of 400 nm to 460 nm which confirms the presence of silver nanoparticles. Figure 9 shows the peak of silver nanoparticles synthesized from marine algae *C. calcitrans*. The absorption spectra obtained by UV-Vis spectroscopy are accurate in confirming the presence of silver nanoparticles since these silver nanoparticles, due to surface plasmon excitation phenomenon in the UV range, show an intense absorption peak. The absorption band of 420 nm is typical for silver nanoparticles. To generate and synthesize nanoparticles with the desired size, shape, and functions, a thorough examination of a component's chemical, physical, and biological properties is needed [20]. The silver nanoparticles were purified, and the

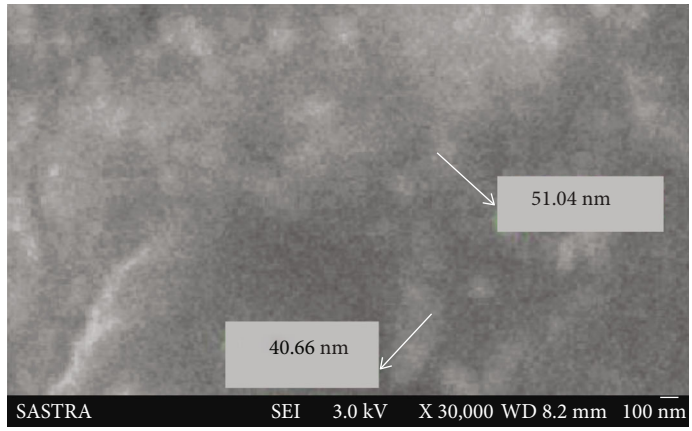

Figure 13: SEM image of nanoparticles with sizes 40 nm and 51 nm.

Figure 14: Silver nanoparticles of sizes from 25 nm to 35 nm, 55 nm to 65 nm, and 85 nm to 95 nm.

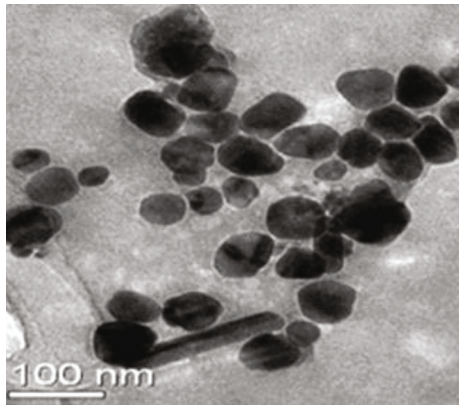

Figure 15: TEM image of silver nanoparticles.

algal cells are removed before the characterization process. If there were any algal cells, they could interfere with the results but were negligible.

The smaller nanoparticles make the band to be around 400 to 450 nm, whereas when the size of silver nanoparticles increases, it could be around 450 nm to 495 nm. The size of nanoparticles has a great impact on the excitation of photons and on the formation of bands. The color change of silver nanoparticles was also greatly influenced by the varied sizes of silver nanoparticles synthesized.

3.5. Scanning Electron Microscopy. The size of the silver nanoparticles synthesized from marine microalgae is examined with the help of a scanning electron microscope (SEM). It is found that the silver nanoparticles synthesized from marine microalgae have a size of 30–80 nm. Figure 10 shows the SEM image of silver nanoparticles with a size of 53.1 nm to 71.9 nm.

The scanning electron microscopy photographs are further taken with various sizes of nanoparticles. Various shapes of silver nanoparticles are found. A number of silver nanoparticles are found with a spherical shape. Cubic, oval, elliptical, and rectangular shapes are some other shapes found in the nanoparticles synthesized from marine microalgae. Figure 11 shows the presence of silver nanoparticles with sizes 33 nm and 39 nm.

Figure 12 shows the nanoparticles with sizes 31 nm, 32 nm, and 36 nm. The different-sized nanoparticles can then be collected separately to carry out various other experiments.

The effect of nanoparticle size on the thermal conductivity of nanoparticles is analyzed by isolating the different sizes of nanoparticles in separate Eppendorf tubes, and then the nanofluids are prepared with various concentrations. The scale used to compare the size of nanoparticles in the SEM image is 100 nm. The magnification of 30,000x is used to capture the different sizes of nanoparticles. 40 nm to 51 nm sized silver nanoparticles are shown in Figure 13.

After taking photographs of silver nanoparticles, it is found to have different ranges of silver nanoparticles. Among the various ranges of sizes in nanoparticles, the separation is done in three categories as 25 nm to 35 nm, 55 nm

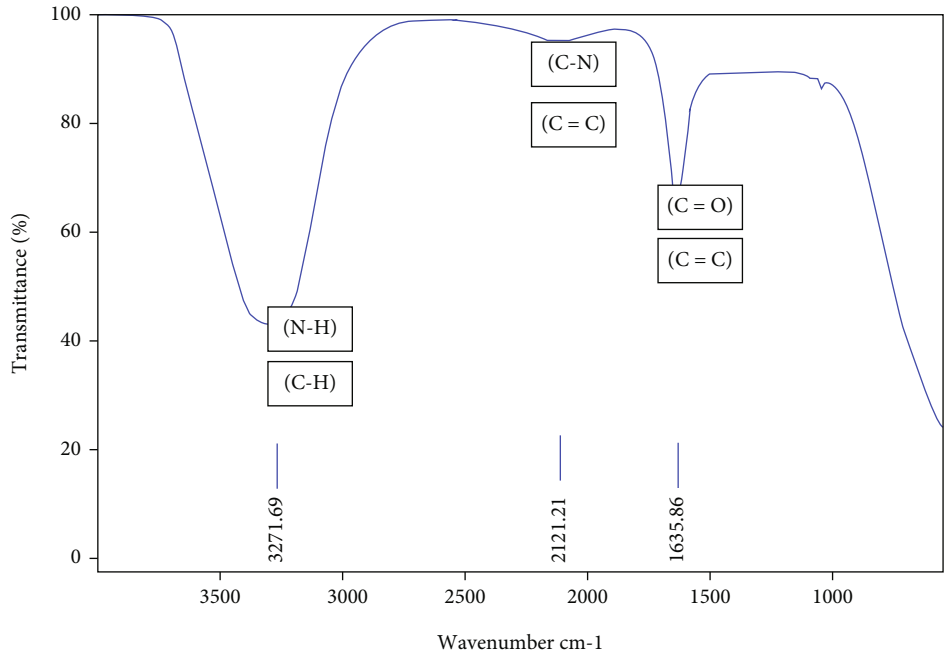

Figure 16: Fourier transform infrared spectroscopy.

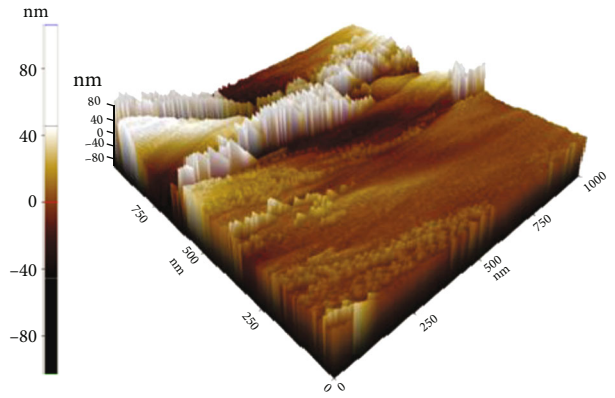

File name	190318Topography006
Head mode	NCAFM
Source	Topography
Data width	256
Data height	256
X scan size	1 um
Y scan size	1 um
Scan rate	0.5 Hz
Z servo gain	1
Set point	13.84 nm
Amplitude	17.74 nm
Set frequency	304.66E3Hz

Figure 17: 3D image of silver nanoparticles by AFM.

to 65 nm, and 85 nm to 95 nm. The powdered samples of different-sized nanoparticles are shown in Figure 14.

3.6. Transmission Electron Microscopy. Transmission electron microscopy analysis gives the data about the size of the particle, the size distribution, and the nanoparticle's morphology. The microscopical method is the only method that is used for measuring the nanoparticle size, where the specific nanoparticles are precisely detected and measured. The data regarding the dispersion of nanoparticles and agglomeration of nanoparticles are obtained using TEM images. Figure 15 illustrates the TEM image of synthesized silver nanoparticles from marine microalgae. The nanoparticles in the range of 20 nm to 99 nm are obtained. The synthesized nanoparticles are well distributed, as obtained from the TEM image taken at high resolution.

3.7. Fourier Transform Infrared Spectroscopy. FTIR analysis of silver nanoparticles was performed in the wavenumber range of 1000-3500 cm^{-1}. The graphs indicate the presence of various chemical groups, and FTIR signals are silver NPs obtained corresponding to C=O vibrations of oxygen, C=C stretching of alkenes (1635 cm^{-1}), then C=C stretching of alkenes (2121 cm^{-1}), N-H stretching of nitrogen groups (3271 cm^{-1}), and N-H stretching of aliphatic groups. These groups suggest the presence of silver NPs. The presence of amino acids is confirmed by the presence of signature peaks which supports the presence of proteins. The bands at positions 1382 and 1035 cm^{-1} are referred to as the vibrations of the C-N stretching of the aromatic and aliphatic amines, respectively. The observations obtained all give the existence and protein binding with that of silver nanoparticles which

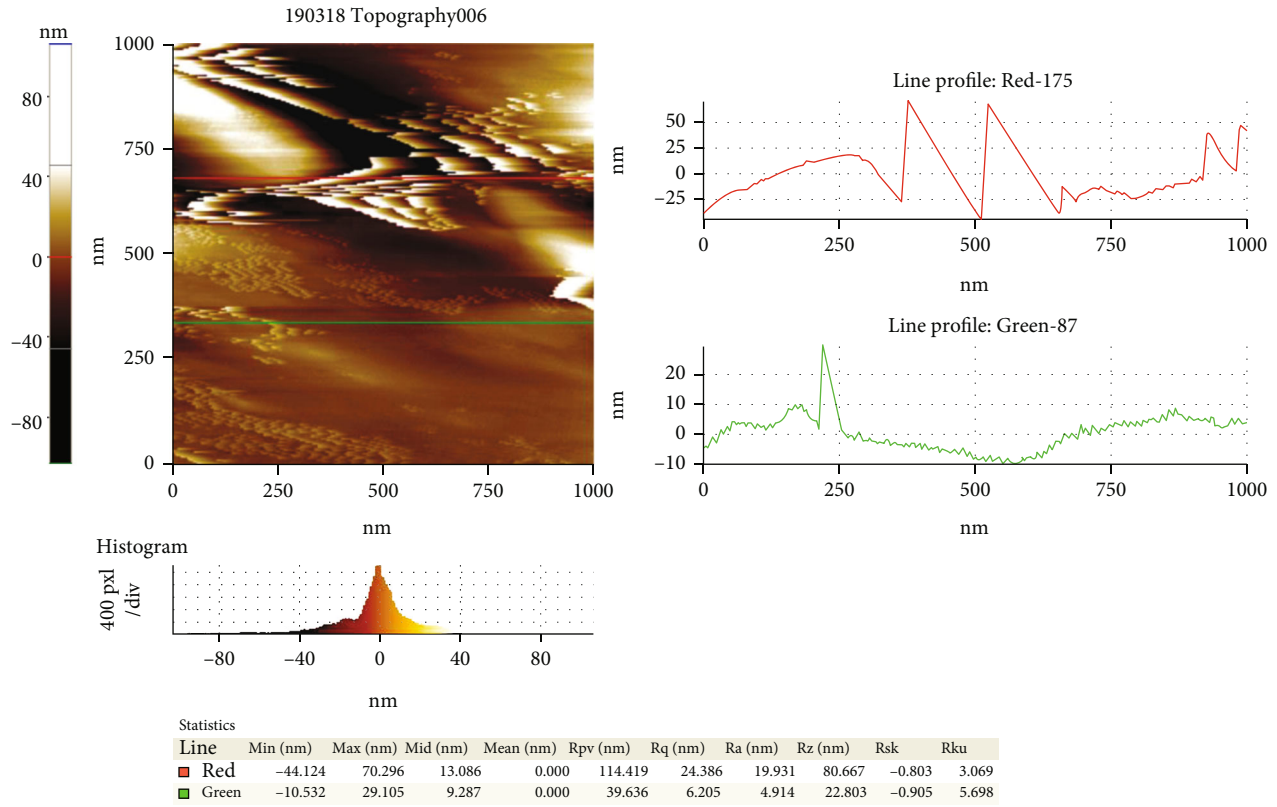

Figure 18: Atomic force microscopy 2D image of silver nanoparticles.

Table 5: Scan details of XRD.

Name	Silver.brml (smooth) #1
Type of scan	Coupled two theta/theta
Mode of scan	Continuous PSD fast
Start	10.002°
End	80.010°
Step size	0.020°
Total time/step	80.00 s
Sample rotation	15.000 1/min
Anode	Cu
Focus orientation	Line focus
Kα1	1.54060 Å
Kα2	1.54439 Å
Kα2 ratio	0.50000
Kβ	1.39222Å
Wavelength for display	1.54060 Å
Generator kV	30.0 kV
Generator mA	10.0 mA
Detector opening	4.850°
Application type	Powder diffraction

leads to stabilization. Also, the FTIR results show that the secondary protein structure did not get disturbed due to the reduction of silver ions to silver nanoparticles. The presence of –OH, C=O, and –CN groups acts as reducing agents in the eco-friendly mode of silver nanoparticle synthesis [21, 22]. Figure 16 shows the FTIR results.

3.8. Atomic Force Microscopy. Atomic force microscopy (AFM) images show the surface topology and size distribution of silver nanoparticles in the solution and also the height and amplitude of the material, as well as the three-dimensional (3D) and two-dimensional (2D) reconstructed images of the general particle. AFM analysis evaluated the presence and size distribution of the generated silver nanoparticles. The scanning area was $1 \times 1\,\mu$m in a tapping mode, and both the three-dimensional (3D) image and the two-dimensional (2D) image are generated in Figures 17 and 18, respectively. The image confirms the uniform distribution of silver nanoparticles. Most of the particles were approximately 40-80 nm in diameter in the sphere topology. The agglomeration of particles to each other can be seen. The average height of the silver nanoparticles is approximately 0-25 nm.

3.9. X-Ray Diffractometry. XRD analysis of prepared silver nanoparticles was done by a powder X-ray diffractometer. The silver nanoparticles synthesized from marine microalgae are powdered for XRD analysis.

The scan details are given in Table 5. The coupled two theta and the continuous PSD fast mode of scan are used in XRD analysis. It started at the range of 10.002° and completed at 80.010°. The type of diffraction carried out in X-ray diffractometry is powder diffraction.

Table 6: Peak details obtained from XRD analysis.

DB compound name	Angle	d value	Net intensity	Gross intensity	Relative intensity	Intensity	FWHM	Width (low)
Peak 1	26.078°	3.41424 Å	201.877	1753.54	18.8%	201.877	0.180	0.090
Peak 2	27.222°	3.27325 Å	95.4102	1671.44	8.9%	95.4102	0.179	0.089
Peak 3	31.710°	2.81947 Å	117.758	1711.09	11.0%	117.758	0.192	0.096
Peak 4	37.583°	2.39128 Å	1072.16	2593.43	100.0%	1072.16	0.295	0.147
Peak 5	43.708°	2.06937 Å	294.951	1562.40	27.5%	294.951	0.325	0.162
Peak 6	63.960°	1.45442 Å	259.275	878.476	24.2%	259.275	0.279	0.140
Peak 7	76.974°	1.23775 Å	231.249	766.864	21.6%	231.249	0.296	0.148

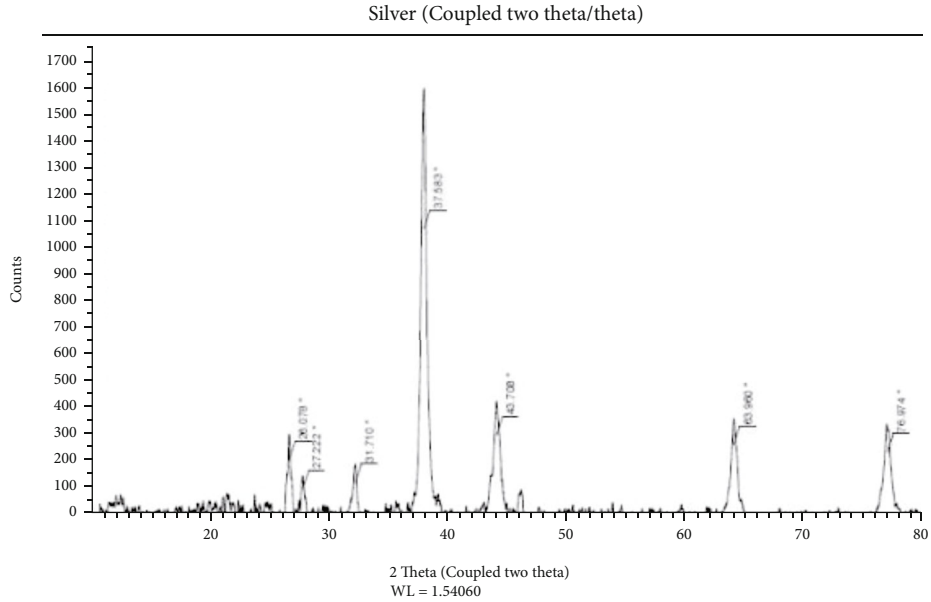

Figure 19: XRD analysis.

The complete peak details of XRD are given in Table 6. The peaks obtained at positions 26.078°, 27.222°, 37.583°, 43.708°, 63.960°, and 75.974° when analyzed confirm the presence of silver nanoparticles. The d value, net intensity, gross intensity, and relative intensity of each peak are obtained and tabulated. The full width at half maximum of peaks is found to be 0.180, 0.179, 0.192, 0.295, 0.325, 0.279, and 0.296 for the seven peaks obtained, respectively. The Bragg reflections obtained indicate the presence of nanoparticles in face-centered cubic form that are crystalline in nature. The peaks that correspond to (111), (121), (200), and (221) correspondingly indicate the presence of silver nanoparticles by XRD analysis.

XRD peaks observed at 26.0, 27.2, 31.7, 37.5, 43.7, 63.9, and 76.9 were related to their corresponding planes. The prepared silver nanoparticle is matched with the ICDD card NO-04-0783. XRD results reveal that the prepared sample is the silver nanoparticles. Silver nanoparticles are formed due to the reduction of $AgNO_3$ into Ag. Bragg's equation was used to calculate the reflection angles in interatomic space [23]. The acquired Bragg reflections revealed that the produced silver nanoparticles are in nanocrystal form and face-centered cubic form and are crystalline in nature when compared to the standard [24]. The excited peaks interpreted by XRD are given in Figure 19.

3.10. Photoluminescence. The photoluminescence of silver nanoparticles is studied to know about the photon excitations. The excitations are done at 350 nm and 400 nm. The peaks obtained due to the photoluminescence of silver nanoparticles are given in Figure 20.

Surface areas of nanoscale materials are far greater than those of comparable masses of larger-scale materials. As a material's surface area per mass increases, more of the material can come into contact with surrounding materials, affecting reactivity. Smaller silver nanoparticles have more reaction sites (where the sites can receive electrons) on their surfaces and are more sensitive to oxygen, a natural electron donor, than larger particles because they have a larger specific surface area.

3.11. Antimicrobial Activity of Silver Nanoparticles against Human Pathogens. The silver nanoparticles synthesized from marine microalgae that are checked for their antimicrobial activity are shown in Table 7. *A. niger*, *Enterobacter spp.*, *E. coli*, *Klebsiella spp.*, *P. vulgaricus*, *P. aeruginosa*, and *S. aureus* are human pathogens used to analyze the antimicrobial activity of silver nanoparticles. Silver nanoparticles synthesized from *C. calcitrans* showed a high zone of inhibition against *P. aeruginosa* and *S. aureus*.

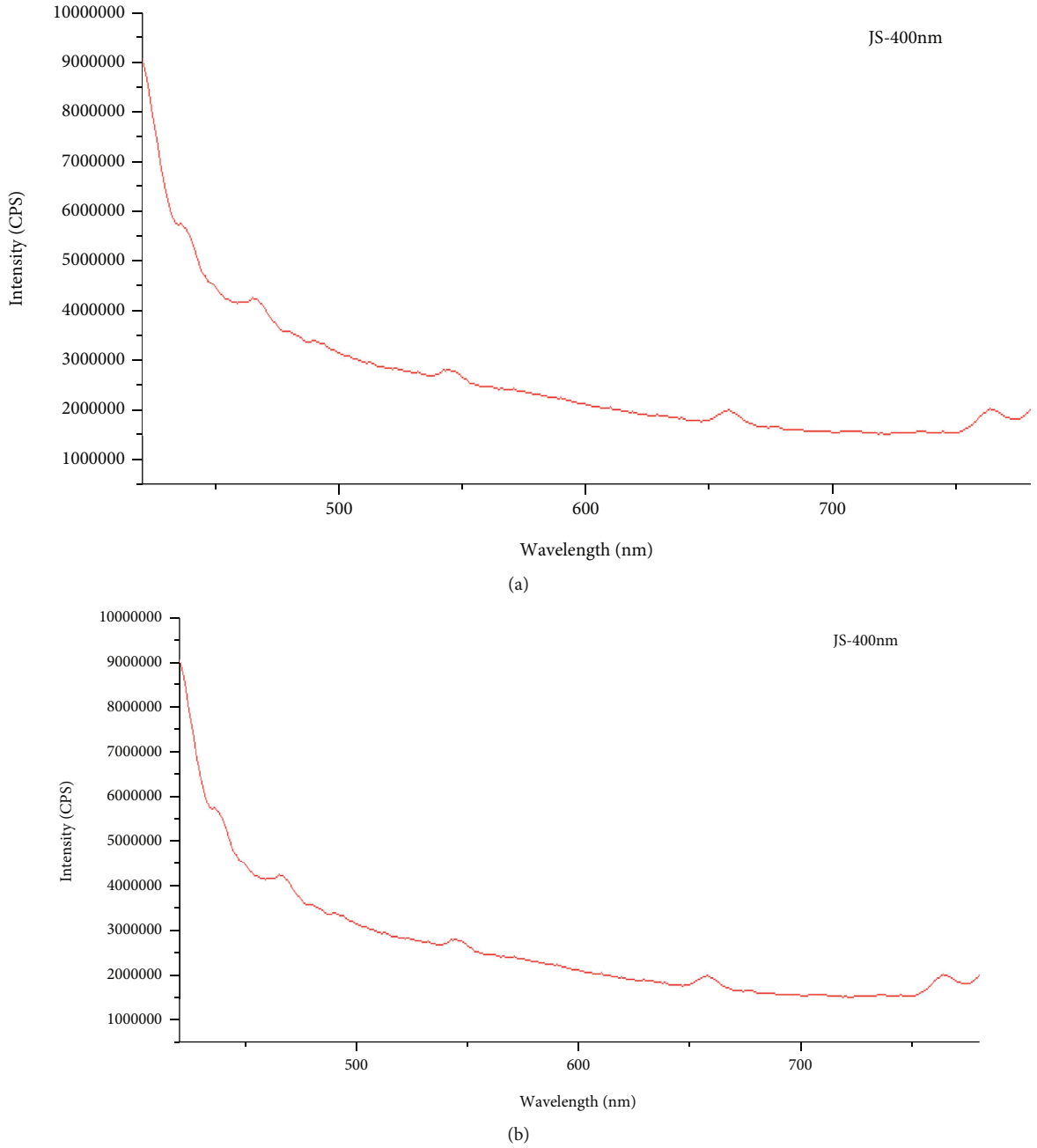

Figure 20: (a) Photoluminescence of silver nanoparticles A at 350 nm. (b) Photoluminescence of silver nanoparticles B at 400 nm.

Table 7: Zone of inhibition of silver nanoparticles against human pathogens.

Organisms	*C. calcitrans*
A. niger	17 mm
Enterobacter spp.	9 mm
E. coli	7 mm
Klebsiella spp.	19 mm
P. vulgaricus	12 mm
P. aeruginosa	18 mm
S. aureus	18 mm

The zone of inhibition shown by silver nanoparticles synthesized from marine microalgae against human pathogens is shown in Figure 21. The silver nanoparticles synthesized from marine microalgae have a high antagonistic character against human pathogens, and hence, these particles can be used in medical applications. Sudha et al. in 2013 investigated the antagonistic nature of algae against human pathogens and analyzed the zone of inhibition [25].

Silver nanoparticles have been imposed as an excellent antimicrobial agent capable of combating bacteria that cause infections in vitro and in vivo. Silver nanoparticles have antibacterial activity against both Gram-negative bacteria and

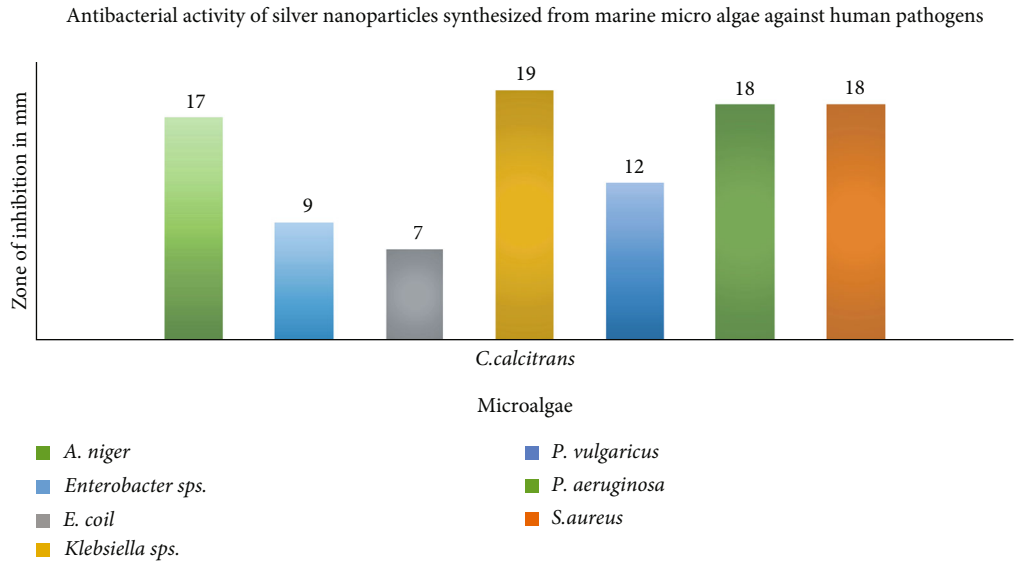

Figure 21: Antimicrobial activity of silver nanoparticles synthesized from marine microalgae against human pathogens.

Gram-positive bacteria, including multidrug-resistant strains. The antimicrobial effect is attributed to positively charged silver ions (Ag+). Silver ions kill microorganisms through a variety of mechanisms. Three major toxicity mechanisms for silver nanoparticles have been suggested: oxidative stress, DNA damage, and cytokine induction. In vivo studies have revealed that exposure to silver nanoparticles can cause effects in a variety of major organs.

The silver nanoparticles' antibacterial activity was compared with commonly available antibiotics gentamicin and streptomycin. It was analyzed that silver nanoparticles have greater potency against bacteria compared with antibiotics. The fold increase in the zone of inhibition was found in discs when silver nanoparticles were impregnated with antibiotics. The mode of action and efficiency were much greater for the wells filled with equal amounts of both silver nanoparticles and antibiotics.

4. Conclusion

Engineering combined with technology made the possibility to achieve a product "silver nanoparticle" in an eco-friendly manner. The marine microalgae are made to grow in Walne's media, and their growth patterns were checked. Value-added silver nanoparticles are synthesized from microalgae at their exponential phase. The characterization of silver nanoparticles with UV-Vis spectroscopy, SEM, TEM, FTIR, XRD, AFM, and PL is done. The antimicrobial activity of silver nanoparticles was analyzed. The silver nanoparticles exhibit high antibacterial activity against human pathogenic organisms.

Data Availability

The datasets generated during and/or analyzed during the current study are available from the corresponding author upon reasonable request.

Conflicts of Interest

The authors declare that they have no conflicts of interest.

References

[1] N. Saifuddin, C. W. Wong, and A. A. Nur Yasumira, "Rapid biosynthesis of silver nanoparticles using culture supernatant of bacteria with microwave irradiation," *E-journal of Chemistry*, vol. 6, no. 1, p. 61, 2009.

[2] H. Huang and X. Yang, "Synthesis of polysaccharide-stabilized gold and silver nanoparticles: a green method," *Journal Carbohydrates Research*, vol. 339, no. 15, pp. 2627–2631, 2004.

[3] A. Ahmad, P. Mukherjee, S. Senapati et al., "*Extracellular biosynthesis of silver nanoparticles using the fungus _Fusarium oxysporum_*," *Colloids and Surfaces B: Biointerfaces*, vol. 28, no. 4, pp. 313–318, 2003.

[4] Y. Zhou, H. Itoh, T. Uemura, K. Naka, and Y. Chujo, "Synthesis of novel stable nanometer-sized metal (M = Pd, Au, Pt) colloids protected by a π-conjugated polymer," *Nanoscience and Nanotechnology Research, Langmuir*, vol. 18, no. 1, pp. 277–283, 2002.

[5] T. Klaus-Joerger, R. Joerger, E. Olsson, and C. G. Granqvist, "Bacteria as workers in the living factory: metal-accumulating bacteria and their potential for materials science," *Trends in Biotechnology*, vol. 19, no. 1, pp. 15–20, 2001.

[6] S. Schultz, D. R. Smith, J. J. Mock, and D. A. Schultz, "Single-target molecule detection with nonbleaching multicolor optical immunolabels," *Proceedings of the National Academy of Sciences*, vol. 97, no. 3, pp. 996–1001, 2000.

[7] M. A. Hayat, *Colloidal Gold: Principles, Methods and Applications*, vol. 1, Academic Press, San Diego, USA, 1989.

[8] K. Simkiss and K. Wilbur, Eds., *Biominerlisation*, Academic press, Elsevier, Availble from: Elsevier books, 2012.

[9] P. K. Stoimenov, R. L. Klinger, G. L. Marchinand, and K. J. Khabude, "Metal oxide nanoparticles as bactericidal agents," *Langmuir*, vol. 18, no. 17, pp. 6679–6686, 2002.

[10] R. Blakemore and P. Ann, "Magnetotactic bacteria," *Annual Review of Microbiology*, vol. 36, no. 1, pp. 217–238, 1982.

[11] N. Kroger, R. Deutzmann, and M. Sumper, "Polycationic peptides from diatom biosilica that direct silica nanosphere formation," *Journal Science*, vol. 286, no. 5442, pp. 1129–1132, 1999.

[12] L. Cepoi, I. Zinicovscaia, R. Ludmila et al., "Effects of PEG-coated silver and gold nanoparticles on Spirulina platensis biomass during its growth in a closed system," *Coatings*, vol. 10, no. 8, pp. 717–732, 2020.

[13] A. V. Miguel, F. Antonio, C. M. Jose, and L. G. Pires Ana, "CO_2 capture using microalgae," in *Advances in Carbon Capture*, Woodhead Publishing, 2020.

[14] D. Devina Merin, S. Praksh, and B. Valentine Bhimba, "Antibacterial screening of silver nanoparticles synthesized by marine micro algae," *Asian Pacific Journal of Tropical Medicine*, vol. 3, no. 10, pp. 797–799, 2010.

[15] R. Nishanthi, S. Malathi, S. John Paul, and P. Palani, "Green synthesis and characterization of bioinspired silver, gold and platinum nanoparticles and evaluation of their synergistic antibacterial activity after combining with different classes of antibiotics," *Materials Science & Engineering C*, vol. 96, pp. 693–707, 2019.

[16] A. K. Genevieve, M. W. Laura, J. F. Sarah, H. Michael, L. P. Amy, and E. O. Janel, "Microwave – assisted green synthesis of silver nanoparticles using orange peel extract," *ACS Sustainable Chemistry & Engineering*, vol. 2, no. 3, pp. 367–376, 2014.

[17] M. Ndikau, N. M. Noah, D. M. Andala, and E. Masika, "Green synthesis and characterization of silver nanoparticles using Citrullus lanatus fruit rind extract," *International Journal of Analytical Chemistry*, vol. 2017, Article ID 8108504, 9 pages, 2017.

[18] H. Safafar, J. Van Wagenen, P. Moller, and C. Jacobsen, "Carotenoids, phenolic compounds and tocopherols contribute to the antioxidative properties of some microalgae species grown on industrial wastewater," *Marine Drugs*, vol. 13, no. 12, pp. 7339–7356, 2015.

[19] R. Anith Jose and P. Jagatheeswari, "Neutroscopic data synthesis of biodegradable polymer for industrial bio robots," *Cognitive Systems Research*, vol. 56, pp. 72–81, 2019.

[20] P. Boomi, R. M. Ganesan, G. Poorani, H. G. Prabu, S. Ravikumar, and J. Jeyakanthan, "Biological synergy of greener gold nanoparticles by using _Coleus aromaticus_ leaf extract," *Materials Science and Engineering*, vol. 99, pp. 202–210, 2019.

[21] K. Gopinath, S. Kumaraguru, K. Bhakyaraj et al., "Green synthesis of silver, gold and silver/gold bimetallic nanoparticles using the _Gloriosa superba_ leaf extract and their antibacterial and antibiofilm activities," *Microbial Pathogenesis*, vol. 101, no. 1, pp. 1–11, 2016.

[22] M. M. J. Gonzalez, M. A. Rodriguez, S. Luque, and J. R. Alvarez, "Recovery of heavy metals from metal industry waste waters by chemical precipitation and nanofiltration," *Desalination*, vol. 200, no. 1-3, pp. 742–744, 2006.

[23] K. Pramila and K. S. Sushil, "Mycogenic nanoparticles and their bio-prospective applications: current status and future challenges," *Journal of Nanostructure in Chemistry*, vol. 8, no. 4, pp. 369–391, 2018.

[24] A. O. Gloria and J. A. Anthony, "*In vitro* antibacterial, antioxidant, and toxicity profile of silver nanoparticles green – synthesized and characterized from aqueous extract of a spice blend formulation," *Biotechnology & Biotechnological Equipment*, vol. 32, no. 3, pp. 724–733, 2018.

[25] S. S. Sudha, K. Rajamanickam, and J. Rengaramanujam, "Microalgae mediated synthesis of silver nanoparticles and their antibacterial activity against pathogenic bacteria," *Indian Journal of Experimental Biology*, vol. 52, pp. 393–399, 2013.

[26] P. Pradeepkumar, R. Naresh Kumar, A. A. Alarfaj, M. A. Murugan, and M. Rajan, "Deep eutectic solvent-mediated FA-g-β-alanine-co-PCL drug carrier for sustainable and site-specific drug delivery," *ACS Applied Bio Materials*, vol. 1, no. 6, pp. 2094–2109, 2018.

[27] A. M. Pradeepkumar, A. H. Elgorban, and M. Rajan, "Natural solvent-assisted synthesis of amphiphilic co-polymeric nanomicelles for prolonged release of camptothecin delivery," *New Journal of Chemistry*, vol. 42, no. 12, pp. 10366–10375, 2018.